Directed Assembly of Discrete Gold Nanoparticle Groupings Using Branched DNA Scaffolds

Shelley A. Claridge, Sarah L. Goh, Jean M. J. Fréchet,* Shara C. Williams, Christine M. Micheel, and A. Paul Alivisatos*

Center for New Directions in Organic Synthesis, University of California, Department of Chemistry, Berkeley, California 94720-1460, and E. O. Lawrence Berkeley National Laboratory, Division of Materials Science, Berkeley, California 94720

Received September 14, 2004. Revised Manuscript Received January 22, 2005

The concept of self-assembled dendrimers is explored for the creation of discrete nanoparticle assemblies. Hybridization of branched DNA trimers and nanoparticle−DNA conjugates results in the synthesis of nanoparticle trimer and tetramer complexes. Multiple tetramer architectures are investigated, utilizing Au−DNA conjugates with varying secondary structural motifs. Hybridization products are analyzed by gel electrophoresis, and discrete bands are observed corresponding to structures with increasing numbers of hybridization events. Samples extracted from each band are analyzed by transmission electron microscopy, and statistics compiled from micrographs are used to compare assembly characteristics for each architecture. Asymmetric structures are also produced in which both 5- and 10-nm Au particles are assembled on branched scaffolds.

Introduction

Current investigations in nanomaterials have identified the need for greater control over the patterning of nanoscale components. The ability to program nanoparticle assemblies may be crucial to characterizing and directing their function.[1,2] Considerable effort has been directed toward investigating the effect of gold nanoparticle placement on the resulting plasmon resonance, since the physical properties of nanoparticles can be strongly influenced by surrounding nanoparticles.[3−6] Neighboring nanoparticles can affect the resonance frequency in a distance-dependent manner, allowing electromagnetic energy to propagate along linear arrays. In this fashion, controlled arrangements of nanoparticles can be used to direct the propagation of light on a length scale smaller than the wavelength of the light itself.[7,8]

Although many synthetic routes to nanoparticles of controlled morphology and composition have been established, the programmed spatial arrangement of nanoparticles remains a challenge. Arrays can be fabricated via atomic force microscopy manipulation or e-beam lithography;[7,8] however, self-assembly provides an attractive alternative if methods can be developed that allow sufficient control over feature size and geometry. Many avenues to self-assembly are currently under investigation, several of which take advantage of macromolecular elements from biological systems.[9−12]

A number of approaches employ the DNA-based assembly of nanoparticles. DNA functionalized with a thiol or amino moiety can undergo facile ligand exchange with citrate- or phosphine-coated gold nanoparticles to give DNA−Au conjugates.[13] Hybridization to a complementary single-stranded oligonucleotide template can then be used to align nanoparticles at defined distances along a single DNA helix.[13−18] Radial assemblies have also been generated by combining two types of nanoparticle conjugates, each bearing multiple copies of complementary single-stranded DNA.[19,20] Larger three-dimensional arrays of programmed DNA have

* To whom correspondence may be addressed. E-mail: frechet@berkeley.edu (J.M.J.F.); alivis@uclink.berkeley.edu (A.P.A.). Tel: (510) 643-3077 (J.M.J.F.); (510) 643-7371 (A.P.A.). Fax: (510) 643-3079 (J.M.J.F.); (510) 642-6911 (A.P.A.).

(1) Xia, Y. N.; Yang, P. D.; Sun, Y. G.; Wu, Y. Y.; Mayers, B.; Gates, B.; Yin, Y. D.; Kim, F.; Yan, Y. Q. *Adv. Mater.* **2003**, *15*, 353−389.
(2) Zhang, Z. L.; Horsch, M. A.; Lamm, M. H.; Glotzer, S. C. *Nano Lett.* **2003**, *3*, 1341−1346.
(3) Kottmann, J. P.; Martin, O. J. F. *Opt. Lett.* **2001**, *26*, 1096−1098.
(4) Sonnichsen, C.; Franzl, T.; Wilk, T.; von Plessen, G.; Feldmann, J. *New J. Phys.* **2002**, *4*, 93.
(5) Storhoff, J. J.; Lazarides, A. A.; Mucic, R. C.; Mirkin, C. A.; Letsinger, R. L.; Schatz, G. C. *J. Am. Chem. Soc.* **2000**, *122*, 4640−4650.
(6) Su, K. H.; Wei, Q. H.; Zhang, X.; Mock, J. J.; Smith, D. R.; Schultz, S. *Nano Lett.* **2003**, *3*, 1087−1090.
(7) Maier, S. A.; Brongersma, M. L.; Kik, P. G.; Meltzer, S.; Requicha, A. A. G.; Atwater, H. A. *Adv. Mater.* **2001**, *13*, 1501−1505.
(8) Maier, S. A.; Brongersma, M. L.; Kik, P. G.; Meltzer, S.; Requicha, A. A. G.; Koel, B. E.; Atwater, H. A. *Adv. Mater.* **2003**, *15*, 562.
(9) Niemeyer, C. M. *Appl. Phys. A: Mater. Sci. Process.* **1999**, *68*, 119−124.
(10) Niemeyer, C. M. *Angew. Chem., Int. Ed.* **2001**, *40*, 4128−4158.
(11) Storhoff, J. J.; Mirkin, C. A. *Chem. Rev.* **1999**, *99*, 1849−1862.
(12) Hooker, J. M.; Kovacs, E. W.; Francis, M. B. *J. Am. Chem. Soc.* **2004**, *126*, 3718−3719.
(13) Loweth, C. J.; Caldwell, W. B.; Peng, X. G.; Alivisatos, A. P.; Schultz, P. G. *Angew. Chem., Int. Ed.* **1999**, *38*, 1808−1812.
(14) Niemeyer, C. M.; Ceyhan, B.; Blohm, D. *Bioconj. Chem.* **1999**, *10*, 708−719.
(15) Alivisatos, A. P.; Johnsson, K. P.; Peng, X. G.; Wilson, T. E.; Loweth, C. J.; Bruchez, M. P.; Schultz, P. G. *Nature* **1996**, *382*, 609−611.
(16) Niemeyer, C. M.; Burger, W.; Peplies, J. *Angew. Chem. Int. Ed.* **1998**, *37*, 2265−2268.
(17) Taton, T. A.; Mucic, R. C.; Mirkin, C. A.; Letsinger, R. L. *J. Am. Chem. Soc.* **2000**, *122*, 6305−6306.
(18) Letsinger, R. L.; Mirkin, C. A.; Elghanian, R.; Mucic, R. C.; Storhoff, J. J. *Phosphorus Sulfur Silicon Relat. Elem.* **1999**, *146*, 359−362.
(19) Niemeyer, C. M.; Ceyhan, B. *Angew. Chem. Int. Ed.* **2001**, *40*, 3685−3688.
(20) Mucic, R. C.; Storhoff, J. J.; Mirkin, C. A.; Letsinger, R. L. *J. Am. Chem. Soc.* **1998**, *120*, 12674−12675.

10.1021/cm0484089 CCC: $30.25
Published on Web 03/09/2005

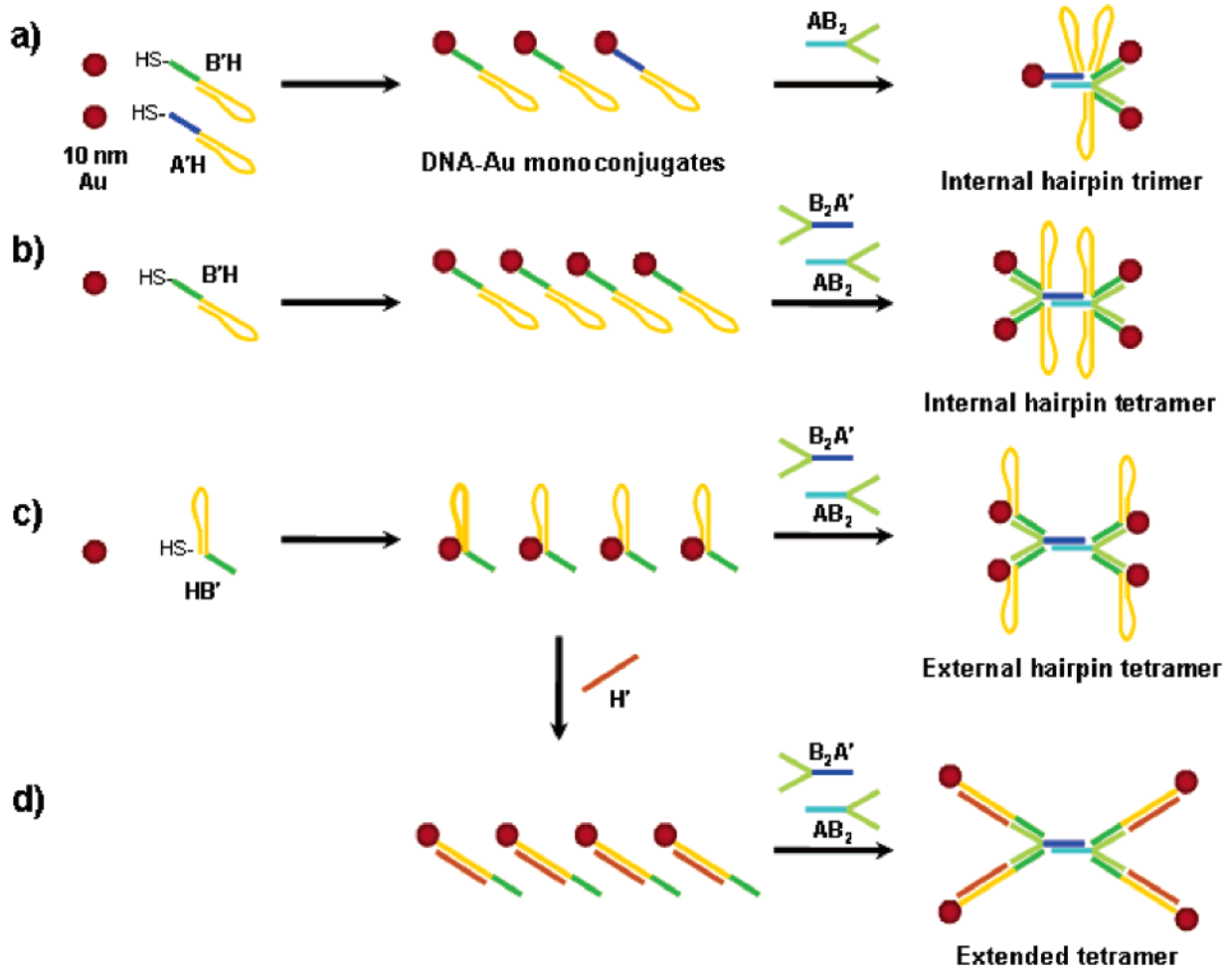

Figure 1. Nanoparticle assemblies using branched DNA scaffolds. Conjugation of gold nanoparticles to thiolated DNA followed by electrophoretic purification yields DNA−Au monoconjugates, which are hybridized with branched scaffolds to yield (a) internal-hairpin trimers, (b) internal-hairpin tetramers, and (c) external-hairpin tetramers. (d) Extended tetramers are formed by adding linear DNA H′ to HB′ monoconjugates prior to hybridization with branched scaffolds.

been prepared by Seeman[21] and Mao and co-workers,[22] and their use as scaffolds is currently under investigation.[23] More complex scaffolds can also be accessed using branched DNA, in which multiple sequences are attached in a nonlinear arrangement. Branched DNA has recently been synthesized using solution-phase coupling[24] as well as variations in solid phase techniques that incorporate the branching unit directly on the support[25,26] or within the DNA sequence. Preliminary studies using statistical conjugates indicate that phosphoramidite branched DNA will be an appropriate scaffold for nanoparticle assemblies.[27]

Controlled conjugation is of primary importance in the formation of discrete DNA-based nanoparticle arrays. Several means to controlled conjugation have been investigated, including electrophoresis,[28] solid-phase methods,[29] and solution-phase extraction based on product solubility.[30] In the electrophoretic protocol used here, conjugation initially results in a statistical mixture of non-, mono-, and polyconjugated Au particles based on the DNA:Au ratio used. Agarose gel electrophoresis of the mixture results in discrete bands corresponding to successive orders of conjugation, if the length of the conjugating DNA is great enough. Previously single-stranded 50-base oligonucleotides have been shown to give discrete bands when conjugated to 5- and 10-nm Au.[28] Bands can then be isolated from the gel, yielding purified conjugates of the desired order.

Here, the DNA-based self-assembly of discrete nanoparticle structures is explored, extending the scope and characterization of this approach with an investigation into the synthesis of gold nanoparticle trimer and tetramer arrangements, illustrated in Figure 1. Since the DNA length required for conjugate purification is greater than the maximum arm length feasible for the synthesis of branched DNA on an

(21) Seeman, N. C. *Angew. Chem., Int. Ed. Engl.* **1998**, *37*, 3220−3238.
(22) Liu, D.; Wang, M. S.; Deng, Z. X.; Walulu, R.; Mao, C. D. *J. Am. Chem. Soc.* **2004**, *126*, 2324−2325.
(23) Xiao, S. J.; Liu, F. R.; Rosen, A. E.; Hainfeld, J. F.; Seeman, N. C.; Musier-Forsyth, K.; Kiehl, R. A. *J. Nanoparticle Res.* **2002**, *4*, 313−317.
(24) Eckardt, L. H.; Naumann, K.; Pankau, W. M.; Rein, M.; Schweitzer, M.; Windhab, N.; von Kiedrowski, G. *Nature* **2002**, *420*, 286.
(25) Scheffler, M.; Dorenbeck, A.; Jordan, S.; Wustefeld, M.; von Kiedrowski, G. *Angew. Chem., Int. Ed. Engl.* **1999**, *38*, 3312−3315.
(26) Shi, J. F.; Bergstrom, D. E. *Angew. Chem., Int. Ed. Engl.* **1997**, *36*, 111−113.
(27) Grimau, M. G.; Iacopino, D.; Avino, A.; de la Torre, B. G.; Ongaro, A.; Fitzmaurice, D.; Wessels, J.; Eritja, R. *Helv. Chim. Acta* **2003**, *86*, 2814−2826.
(28) Zanchet, D.; Micheel, C. M.; Parak, W. J.; Gerion, D.; Alivisatos, A. P. *Nano Lett.* **2001**, *1*, 32−35.
(29) Sung, K. M.; Mosley, D. W.; Peelle, B. R.; Zhang, S. G.; Jacobson, J. M. *J. Am. Chem. Soc.* **2004**, *126*, 5064−5065.
(30) Jhaveri, S. D.; Foos, E. E.; Lowy, D. A.; Chang, E. L.; Snow, A. W.; Ancona, M. G. *Nano Lett.* **2004**, *4*, 737−740.

automated synthesizer, two hybridization strategies are pursued. In the first design, the excess bases on the 50-base conjugate form a hairpin loop near the branch point, decreasing the maximum distance between nanoparticles in a single structure. In the second strategy, excess conjugate bases are moved to the exterior of the structure. This eliminates the possible steric issues caused by multiple tails at the branch point and allows formation of extended structures, which can potentially act as the basis of a switchable system if scaffold and conjugates are cross-linked covalently. Hybridized structures are separated by gel electrophoresis, resulting in discrete bands that are extracted and analyzed by transmission electron microscopy (TEM). Band identities are suggested based on the number of hybridization events, and statistics and images from TEM analysis are provided to support the validity of the proposed structure. Such self-assembled arrangements represent a first step toward accessing complex arrays of nanoparticles with multiple branch points and nanoparticle sizes.

Materials and Methods

General Procedures. Citrate-coated 5- and 10-nm gold particles with <10% deviation in diameter were purchased from Ted Pella (Redding, CA). In these solutions, nanoparticle concentrations were approximately 80 nM for the 5-nm particles and 10 nM for 10-nm particles. The bis(*p*-sulfonatophenyl)phenylphosphine dihydrate dipotassium ligand used to stabilize the nanoparticles in aqueous solutions was obtained from Strem Chemicals (Newburyport, MA). DNA purified by polyacrylamide gel electrophoresis (PAGE), thiolated and nonthiolated **HA′**, **A′H**, **B′H**, **C′N**, and **H′**, was purchased from Integrated DNA Technologies (Coralville, IA) and resuspended in deionized water to a final concentration of 50−100 μM. Branched scaffolds were used at working concentrations of 1−2 μM. Nanoparticle sample purification and concentration were carried out in a Fisher Marathon 8K benchtop centrifuge. UV−vis absorption measurements were taken using a Perkin-Elmer Lambda 35 spectrometer. In all protocols specifying 50 mM NaCl, one-fourth volume of a solution of 250 mM NaCl was used to achieve a final concentration of 50 mM.

TEM was performed using the Phillips Tecnai 12 instrument at the Electron Microscopy Laboratory at the University of California, Berkeley, CA, with samples visualized at a magnification of 87k. Carbon-coated copper TEM grids (Ted Pella) were prepared according to modified literature procedure[31] described briefly here: 5 μL of dilute aqueous sample was spotted onto a grid and left for 90 s before lightly touching one edge of the grid to filter paper to wick off moisture. Grids were then allowed to air dry prior to analysis.

Electrophoresis of Au−DNA Conjugates and Nanoparticle Assemblies. Gels were prepared with 3% agarose by weight in 0.5X Tris-Borate-EDTA (TBE) buffer. Samples were diluted with 3X loading buffer containing 15% Ficoll 400 (Fluka, Milwaukee, WI) and then loaded into the appropriate well. Gels were run at 5 V/cm for 90 min and then visualized under white light using an Eagle Eye II CCD and EagleSight 2.2 software from Stratagene (La Jolla, CA) or a GelDoc gel imaging system from UVP (Upland, CA).

Synthesis of Branched DNA. Branched DNA was synthesized in the 3′ to 5′ direction on solid phase on a 1-μmol scale using an Expedite 8909 DNA synthesizer (Applied Biosystems, Foster City, CA) with A^{Pac}, $G^{iPr-Pac}$, C^{Ac}, and T (UltraMILD) phosphoramidites from Glen Research Corporation (Sterling, VA). A symmetric doubler phosphoramidite available from Glen Research was used to introduce the branch point; the standard synthesizer protocol was modified to allow a 15-min coupling time for the doubler phosphoramidite. DNA was purified by 10% denaturing polyacrylamide gel electrophoresis.[32] The identity of the trimers was confirmed with matrix-assisted laser desorption ionization time-of-flight (MALDI-TOF) mass spectrometry using a PerSeptive Biosystems Voyager-DE instrument in negative ion mode, with samples crystallized in a matrix of 0.35 M 3-hydroxypicolinic acid (HPA)[33] and 0.1 M ammonium citrate in a 2:1 mixture of CH_3CN and H_2O. MALDI-TOF MS: (*m*/*z*) **AB_2** calcd.: 16 962 (M−H). Found: 16 897. **$A'B_2$** calcd.: 16 972 (M−H). Found: 16 964. **AC_2** calcd.: 16 892 (M−H). Found: 16 874.

Synthesis of Gold−DNA Conjugates. Gold samples were prepared following literature procedure.[13] To 100 mL of citrate-coated gold nanoparticle solution, 60 mg of bis(*p*-sulfonatophenyl)-phenylphosphine dihydrate dipotassium salt was added, and the mixture was stirred at room temperature in order to allow phosphine ligands to replace the citrate ligands. Following overnight incubation, NaCl was added to the stirring mixture until a color change from red to cloudy purple was observed. The solution was transferred to 50-mL centrifuge tubes and centrifuged at room temperature for 15 min at 3 000 rpm to collect the precipitated gold. The supernatant was removed, and the pellet was resuspended in approximately 1 mL of phosphine buffer (1 mg of bis(*p*-sulfonatophenyl)phenylphosphine in 1 mL of deionized water). Samples were then concentrated at room temperature using 50k MWCO Centricon centrifugal concentrators (Millipore, Billerica, MA) for 5−15 min at 3 000 rpm, to a final nanoparticle concentration of 5.0−10.0 μM for 5-nm Au particles and 1.0−1.5 μM for 10-nm particles. Nanoparticles and Au−DNA conjugates were quantified by measuring the absorbance at $\lambda = 520$ nm and calculating the concentration using Beer's law based on their extinction coefficients: $\epsilon_{520}(5\text{ nm}) = 9.3 \times 10^6\ M^{-1}\ cm^{-1}$ and $\epsilon_{520}(10\text{ nm}) = 8.1 \times 10^7\ M^{-1}\ cm^{-1}$.

To prepare Au−DNA conjugates, 3′- or 5′-thiolated DNA was mixed with concentrated gold colloids in a molar ratio chosen to maximize the monoconjugate yield, typically 0.5−2.0 DNA:Au. A final concentration of 50 mM NaCl was achieved using a solution of 250 mM NaCl, and the mixture was incubated at room temperature for 1 h before adding one-fifth volume 15% Ficoll loading buffer and loading into agarose gels.

For 5-nm Au conjugates, sufficient sample was added to achieve a loading of 120 pmol of Au per lane; for 10-nm conjugates, a loading of 20 pmol of Au per lane was used. After 90 min of electrophoresis, gels were cut downstream of the monoconjugate band, and glass fiber filter paper and 10k MWCO dialysis membranes were inserted. After a further 7−9 min of gel electrophoresis, the desired band entered the filter paper and was stopped by the dialysis membrane. The filter paper was removed and the sample eluted by centrifuging with a 0.22-μm centrifugal filter. The sample was then further concentrated using 50k MWCO Centricon centrifugal filters at room temperature for 5−10 min at 2 500 rpm to a final conjugate concentration of approximately 2.0 μM for conjugates of 5-nm Au particles and approximately 0.5 μM for conjugates of 10-nm particles. Concentrated conjugate was collected

(31) Zanchet, D.; Micheel, C. M.; Parak, W. J.; Gerion, D.; Williams, S. C.; Alivisatos, A. P. *J. Phys. Chem. B* **2002**, *106*, 11758−11763.

(32) Sambrook, J.; Fritsch, E. F.; Maniatis, T. Gel Electrophoresis of DNA. In *Molecular Cloning: A Laboratory Manual*; Nolan, C., Ferguson, M., Eds.; Cold Spring Harbor Laboratory Press: Plainview, 1989; pp 6.1−6.62.

(33) Wu, K. J.; Steding, A.; Becker, C. H. *Rapid Commun. Mass Spectrom.* **1993**, *7*, 142−146.

Table 1. DNA Sequences for the Synthesis of Nanoparticle Assemblies

strand	DNA sequence (3−5)[a,b,c]
HA′	*CCC GAG TT*C TGA TGT TTA CGC TT*A ACT TGG G*CC AGT GTA TCG CAA TGA CG-SH
HB′	HS-*CCC GAG TT*C TGA TGT TTA CGC TT*A ACT TGG G*CT GAC AGG TCC AAA GCA CG
B′H	HS-TGA CAG GTC CAA AGC ACG *CCC GAG TT*C TGA TGT TTA CGC TT*A ACT TGG GC*
C′N	HS-GTT GTA GGA GCT TGC TCG ATT GAC TGT TAC ATG AGG TAC TAG CTG AAG TG
H	GCC CAA GTT AAG CGT AAA CAT CAG AAC TCG GG
AB_2	CGT CAT TGC GAT ACA CTG-X-(CGT GCT TTG GAC CTG TCA)$_2$
AB_2	CAG TGT ATC GCA ATG ACG-X-(CGT GCT TTG GAC CTG TCA)$_2$
AC_2	CGT CAT TGC GAT ACA CTG-X-(CGA GCA AGC TCC TAC AAC)$_2$

[a] Underlined bases hybridize with the arm of a branched trimer. [b] Italicized bases undergo hybridization to form the hairpin. [c] X = branch point.

from the top of the filter and quantified by measuring the absorption at 520 nm.

Synthesis of Internal Hairpin Au−DNA Trimer. Au−DNA conjugates Au−**HA′** and Au−**B′H** bearing 10-nm gold particles were mixed with the branched trimer $\mathbf{AB_2}$ in 50 mM NaCl. The mixture was heated briefly to 75 °C to ensure complete melting of the DNA strands and then allowed to cool slowly to room temperature overnight in order to form stable duplexes. Typically, a 1.5-fold molar excess of conjugates was used in order to maximize the number of hybridized structures. Following overnight incubation, the sample was analyzed by agarose gel electrophoresis. Bands were isolated using the filter paper and dialysis membrane procedure described for the Au−DNA conjugates.

Synthesis of Internal Hairpin Au−DNA Tetramer. To prepare the symmetric tetramer, the DNA trimers $\mathbf{AB_2}$ and $\mathbf{A'B_2}$ were hybridized with 6 equiv of 10-nm Au−**B′H** conjugate in 50 mM NaCl using the hybridization protocol described for the trimer synthesis. Gel electrophoresis was also performed as described previously, and the sample was extracted using a crush and soak procedure in which each band was cut out, finely chopped, and gently agitated in 50 μL of 0.5X TBE for 5 min prior to preparation of TEM grids.

Synthesis of External Hairpin and Extended Au−DNA Tetramers. Symmetric external hairpin and extended Au−DNA tetramers were prepared and extracted as described for the internal hairpin tetramer. In this case, trimers $\mathbf{AB_2}$ and $\mathbf{A'B_2}$ were hybridized with 6 equiv of 10-nm Au−**HB′** conjugate and 0 or 12 equiv of **H′** for external hairpin and extended structures, respectively.

Synthesis of Asymmetric Au−DNA Structures. Branched scaffold $\mathbf{AB_2}$, 10-nm Au−**HA′** conjugate, and 5-nm Au−**B′H** conjugate were hybridized to generate the asymmetric trimer, using approximately a 1.5-fold molar excess of conjugate per binding site. Asymmetric tetramers were prepared by incubating $\mathbf{AC_2}$, $\mathbf{A'B_2}$, 10-nm Au−**C′N**, and 5-nm Au−**B′H** in a 1:1:4:4 molar ratio. Incubation, electrophoretic analysis, and TEM were performed as described above.

Statistics. Statistical analysis was performed on micrographs from each grid using either literature procedure[31] or visual inspection to determine the percentage of particles participating in tetramer, trimer, dimer, and other groupings. Micrographs were first evaluated by Image Pro Plus graphics analysis software (Media Cybernetics, Inc.) to maximize the contrast between the particles and background. The number and distance between particles were counted, and the resulting data analyzed using a Labview (National Instruments) program. A particle was considered to be part of a tetramer if three and only three other particles were within an appropriate distance for connection via the DNA scaffold, approximately 30 nm for internal hairpin tetramers and 55 nm for external hairpin and extended tetramers. This distance is calculated to be the sum of the lengths of the three scaffold arms, the length of the branch points, twice the length of the six-carbon thiolating linker, and twice the radius of the gold particles. For internal hairpin trimers, the same criteria were applied to groups of three particles; distance calculations assuming a single scaffold give a diameter of approximately 20 nm. It should be noted that, although each 18-base hybridizing arm is shorter than the persistence length of helical DNA,[34,35] the conformational flexibility at the branch points of the scaffold and at the thiol attachment points make it possible for all particles in a hybridized structure to lie in contact with one another. Tetramer diameters were also evaluated using Image Pro Plus software, taking the diameter of a structure to be the maximum distance between particle centers.

Results and Discussion

Design of Self-Assembled Au−DNA Complexes. Gold nanoparticles were arranged on a DNA scaffold to generate both symmetric and asymmetric trimers and tetramers as illustrated in Figure 1. The branched DNA was synthesized on a solid phase in the 3′ to 5′ direction to produce a three-armed dendritic structure comprised of one unique and two duplicate sequences. To generate well-defined assemblies, gold nanoparticles functionalized with a single complementary DNA sequence were utilized. Previous studies in the Alivisatos and Schultz groups have shown that mixing 5- or 10-nm Au particles with thiolated DNA produces a statistical mixture of mono- and polyconjugates but that monoconjugated gold can be purified by agarose gel electrophoresis if a sufficiently long DNA sequence is used for conjugation.[13,15,28,31,36] Use of 50-base single-stranded oligonucleotides allows for adequate separation of conjugates of both 5- and 10-nm Au particles. Two of the DNA sequences used for conjugation contained a hairpin-forming sequence, which could be expected to reduce band separation by reducing the size of the conjugate; however, band separation was still adequate for monoconjugate isolation. Because of the directionality inherent in the synthesis of the DNA trimer, Au−DNA conjugates were synthesized with either a 3′ or 5′ thiol attachment, as necessary.

DNA sequences were designed to minimize competitive binding events between strands. The arm length of the dendritic DNA was chosen so as to give a melting temperature above room temperature for stable duplex formation ($T_m \approx 60$ °C) while accommodating the pore size of the solid support. In the following discussions, sequences are labeled as **A**, **B**, etc., with the sequences given in Table 1. $\mathbf{AB_2}$ refers to a branched DNA trimer having one **A** and two **B** arms. **A′** denotes a sequence complementary to **A**. The portion of

(34) Bloomfield, V. A.; Crothers, D. M.; Tinoco, I., Jr. *Physical Chemistry of Nucleic Acids*; Harper & Row: New York, 1974.
(35) Viovy, J. L. *Rev. Mod. Phys.* **2000**, *72*, 813−872.
(36) Parak, W. J.; Pellegrino, T.; Micheel, C. M.; Gerion, D.; Williams, S. C.; Alivisatos, A. P. *Nano Lett.* **2003**, *3*, 33−36.

the conjugate sequence not hybridizing to the scaffold, labeled **H**, formed a hairpin loop with either 8 or 9 hybridizing bases on each end and a T_m of approximately 50 °C.

Internal hairpin structures were formed from conjugates in which the hairpin sequence was positioned near the branch point of the scaffold; for external hairpin and extended structures, the hairpin sequence was proximal to the nanoparticle, placing it at the exterior edge of the scaffold. In the extended architecture, linear unthiolated sequence **H′** was also added to prevent hairpin formation. For asymmetric structures, a nonhybridizing tail of sequence **N** was used.

Synthesis and Characterization of a Symmetric 10-nm Au−DNA Trimer. Characterization of nanoparticle trimers provides a simple model of the behavior of nanoparticle assemblies on branched scaffolds. Gold nanoparticle trimers with conjugate hairpins near the branch point were prepared using the **AB$_2$** DNA trimer and **HA′** and **B′H** monoconjugated 10-nm Au particles. The reaction mixture was analyzed using gel electrophoresis as shown in Figure 2a. In the gel, free gold colloid and monoconjugated 10-nm gold were run as standards in lanes 1 and 2, respectively. Varying volumes of trimer reaction mixture were loaded in different lanes, corresponding to gold nanoparticle loadings from 2 to 8 pmol, to allow for simultaneous visualization of bands with differing intensities. For example, band 5 only becomes clearly visible with high loading in lane 5, while bands 2 and 3 blur together at this loading and are only visible as distinct bands at lower loadings as in lane 3.

Although DNA hybridization is inherently both specific and stable, a mixture of hybridization products is found, as seen in lanes 3−5. Since bands are detected visually based on the presence of the highly colored gold colloid, there is no band corresponding to unhybridized branched DNA. The five remaining possibilities for statistical hybridization are pictured below the gel in Figure 2a. The free gold and monoconjugate standards provide positive identification of bands 1 and 2. Structures with increasing numbers of nanoparticles and amounts of DNA are expected to exhibit reduced mobilities since their larger size slows progress through the pores of the gel. Thus bands 3−5 are assigned to structures corresponding to one, two, and three hybridization events, respectively. The relative retention of each band is calculated as a ratio of the band migration to that of free 10-nm gold. On the basis of the band-structure correlations above, a fully formed trimer was found to have a retention of 0.44.

Samples isolated from each band were analyzed via TEM. Representative micrographs from bands 2−5 are shown in Figure 2b. According to the suggested band assignments, structures isolated from bands 2 and 3 should each contain a single nanoparticle, while those from bands 4 and 5 should contain dimers and trimers, respectively. Visual inspection of the nanoparticle groupings in the micrographs supports these assignments, and compiled statistics demonstrate that band 5 contains the highest percentage of particles participating in trimer groupings.

Synthesis and Characterization of Three Symmetric 10-nm Au−DNA Tetramers. Having successfully synthesized

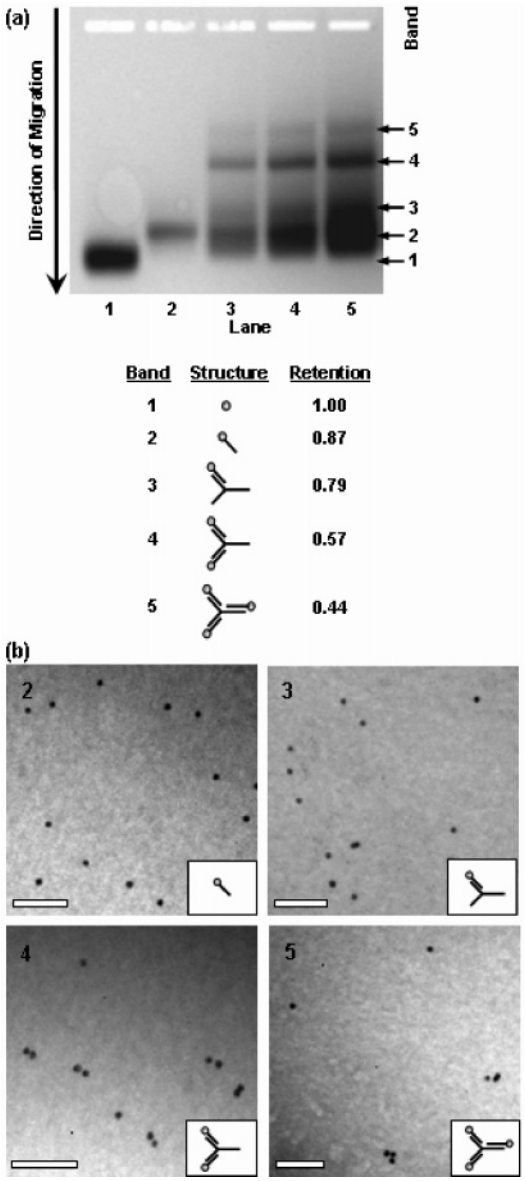

Figure 2. Analysis of internal-hairpin trimer hybridization products by (a) agarose gel electrophoresis and (b) TEM. (a) Lane 1, 10-nm gold; lane 2, 10-nm HB′ conjugate; lanes 3−5: 10-nm trimer mixture, loaded by conjugate content, with 2, 4, and 8 pmol of Au−DNA per lane. (b) Transmission electron micrographs, labeled by band number and suggested structure. Scale bar = 100 nm.

and purified gold nanoparticle trimers using a branched DNA scaffold, this approach was elaborated using two complementary branched DNA trimers to provide a more complex scaffold. Three versions of the tetramer architecture were explored. Two branched scaffolds **AB$_2$** and **A′B$_2$** were prepared and hybridized with appropriate conjugates to form the three tetramer structures shown in Figure 1: Au−**B′H** to generate the internal hairpin tetramer, Au−**HB′** for the external hairpin, and both Au−**HB′** and **H′** for the extended structure. Each design has a different potential benefit: internal hairpins guarantee a small distance between nanoparticles in a single structure; external hairpins likely provide similar particle spacing but without the potential steric issues caused by hairpins near the branch point; addition of complementary DNA to linearize the hairpin is expected to increase interparticle distances but may facilitate conjugate hybridization since the hybridizing sequence will not be

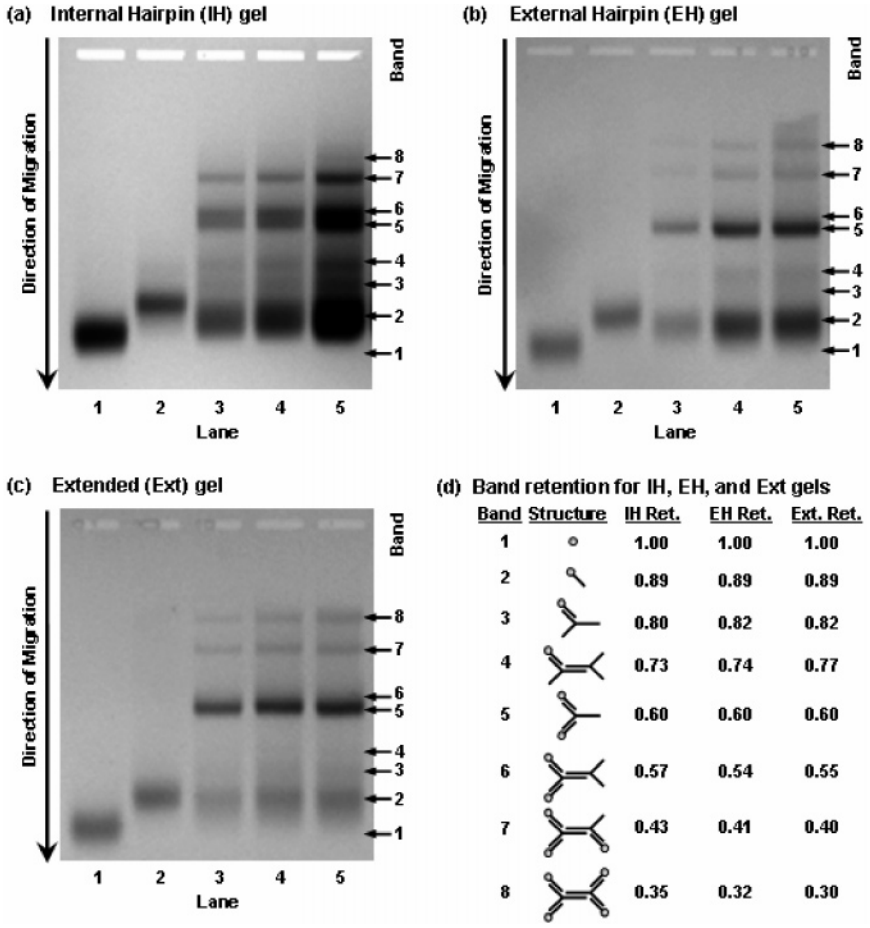

Figure 3. Electrophoretic analysis of tetramer hybridization products for (a) internal-hairpin, (b) external-hairpin, and (c) extended structures. Lane 1, 10-nm gold; lane 2, 10-nm **B′H** conjugate; lanes 3−5, 10-nm tetramer mixture, loaded by conjugate content, with 2, 4, and 8 pmol of Au−DNA per lane in (a), and 1.5, 2.5, and 5 pmol of Au−DNA per lane in (b) and (c). Retention values (d) are calculated for each band as the band migration relative to the migration of the free gold standard in that gel.

folded back toward the nanoparticle surface. In addition, the external hairpin and extended structures could be developed as a bistable or "switchable" system in which the interparticle distance could be varied with temperature or with the addition of the **H′** extending sequence. This functionality would rely on the covalent cross-linking of scaffold to scaffold and scaffold to conjugate, since the melting temperatures of the 18-base scaffold arms and the hairpin sequence are similar.

Hybridization products were analyzed by agarose gel electrophoresis (Figure 3), and band retentions for the internal hairpin tetramer architecture were compared with those for the internal hairpin trimer. Electrophoretic analysis of the tetramer hybridization yielded more bands than trimer hybridization, which was expected since tetramer hybridization affords a larger number of possible structures. Visible bands are believed to correspond to the eight structures shown in Figure 3d, with the identities of bands 1 and 2 again confirmed by the migration of the free gold and conjugate standards. Retention values for each band were calculated relative to the free gold standard. Retention values of bands 3 and 5 in the tetramer gel (0.80 and 0.60, respectively) are comparable with those of bands 3 and 4 of the trimer hybridization gel (0.79 and 0.57), as would be expected for identical single-scaffold monomer and dimer structures. The retention of tetramer band 6 (0.57 for the internal hairpin structure) is also comparable to that of trimer band 4, so an additional experiment was performed to show that tetramer bands 5 and 6 indeed correspond to the single- and double-scaffold dimers, respectively (see Supporting Information). Retentions for tetramer band 7 (0.43) and trimer band 5 (0.44), both assigned as structures containing three nanoparticles, were quite similar despite the extra DNA scaffold in the structure from the tetramer hybridization. This implies that the number of nanoparticles is more important than the quantity of DNA present in a structure, in determining the rate of migration through the gel. An analogous case is bands 5 (single-scaffold dimer), 6 (double-scaffold dimer), and 7 (trimer) in the tetramer gel: structures in bands 5 and 6 differ by a branched scaffold and have almost identical retentions ($\Delta = 0.03$), whereas bands 5 and 7 differ by addition of a nanoparticle conjugate and have a more substantial difference in retention ($\Delta = 0.17$).

Comparison of retention values across the three-tetramer architectures shows that bands are similarly retained even with differences in structure organization. One likely explanation is that structures migrate through the gel in a partially collapsed form, in agreement with previous findings for the behavior of Au−DNA conjugates.[31] Thus, little difference is expected when comparing the migrations of internal hairpin structures to those of external hairpin structures.

Visual analysis of band optical densities reveals that, in both outside-hairpin and extended structures, the desired

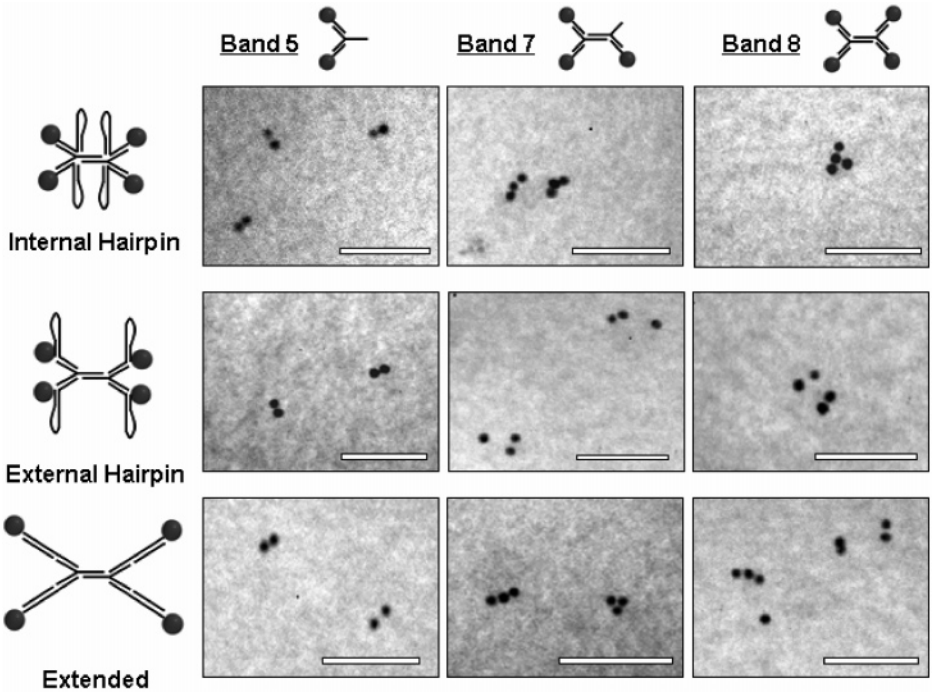

Figure 4. Transmission electron micrographs of sample extracted from dimer, trimer, and tetramer bands in each gel shown in Figure 3. Scale bar = 100 nm.

tetramer structure (band 8) is formed in significantly higher yield than for the inside-hairpin structure. While band 8 is extremely faint in the inside-hairpin gel even at high sample loadings (8 pmol Au−DNA conjugate), it is clearly visible in both external hairpin and extended gels at much lower loading (2.5 pmol). Further, the increased percentage of conjugate hybridization (reduced band 2 intensity) in the extended structure gel implies that straightening of the hairpin facilitates scaffold−conjugate hybridization. In both outside-hairpin and extended hybridizations, single-scaffold dimers appear to be the primary product, suggesting that the central arm of the tetramer is the weak link in both the external-hairpin and extended structures. Ongoing experiments involve exploration of methods for increasing the extent and stability of central arm hybridization, including covalent cross-linking and modification of the central arm sequence. Realizing this goal should greatly increase tetramer yields, which are currently quite low.

Transmission electron micrographs were used to evaluate nanoparticle organization in tetramer hybridization samples before and after electrophoretic purification. Statistical analysis of TEM micrographs from an unpurified external-hairpin hybridization sample shows nanoparticles participate in groupings in ratios that appear to correlate with the optical densities of the bands observed in the gel: 38% monomer, 33% dimer, 20% trimer, and 9% tetramer (excluding 11% higher-order aggregates). Micrographs of samples extracted from hybridization gels again support the assertion that bands with decreasing mobility correlate to increasing numbers of hybridization events (Figure 4 and Supporting Information). Since both the scaffold branch points and thiol attachment points are flexible, a number of different tetramer conformations are observed, as shown in Figure 5. Statistics compiled from the full set of micrographs of each sample (see Supporting Information) show that, for external-hairpin and

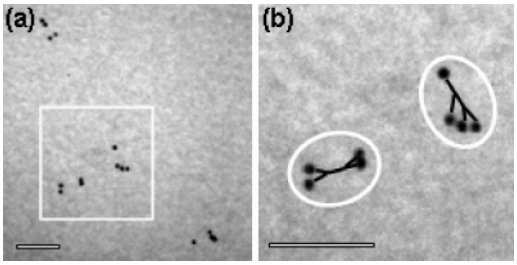

Figure 5. (a) Transmission electron micrograph of sample extracted from tetramer band in the extended tetramer gel shown in Figure 3c. (b) Because of the flexibility of the branch points of the scaffold and the thiol linkers, multiple tetramer conformations may be observed. Scale bar = 100 nm.

extended structures, approximately 60−75% of the particles participate in their predicted grouping. For internal-hairpin samples, statistics were less conclusive, suggesting that the steric factors introduced by the hairpin near the branch point decrease structure stability. Since a small number of monomers and high-order aggregates were observed in micrographs from most grids, it is believed that some amount of structural reorganization is induced by the extraction and grid preparation processes; however, the extent of reorganization is far greater in the internal-hairpin samples. Importantly, the large majority of particles participating in a single-structure type per band in both external-hairpin and extended structures seems to indicate that each discrete band initially contains structures of a single type and that optimization of the extraction procedure will yield samples of pure dimers, trimers, and tetramers.

Diameters were determined for all tetramers extracted from band 8 of the extended and external-hairpin hybridization gels, with the diameter taken to be the maximum distance between centers of two particles in a single grouping. Theoretical maximum diameters were calculated to be 55 and 32 nm, respectively, for the extended and external-hairpin structures, assuming that hairpins remained intact and flexible

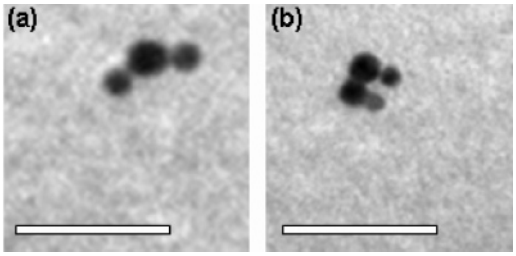

Figure 6. Transmission electron micrographs of (a) asymmetric 5- and 10-nm trimers and (b) asymmetric 5- and 10-nm tetramers. Scale bar = 50 nm.

points adopt their most extended configurations. Observed mean diameters were found to be 44 and 35 nm, with a significant number of diameters within 1 nm of each calculated maximum. Although the mean diameter of the extended structure is greater than that of the external hairpin as expected, it is also well below the theoretical maximum. This result is not unreasonable given that a nick near the midpoint of each arm allows considerable rotation, which can only decrease the interparticle distances. For the external-hairpin structure, 46% of the diameters were within 1 nm of the calculated maximum for a structure with intact hairpins. However, 30% of the diameters were also between the calculated maxima for the intact external hairpin and the extended structures, suggesting that one or more of the four hairpins may partially unwind, allowing the conjugated gold particle to move farther from the others in the structure.

Expanding the Synthetic Capabilities: Asymmetric Assemblies. The asymmetric nature of the branched DNA scaffold was further exploited for the synthesis of self-assembled asymmetric trimer and tetramer structures containing both 5- and 10-nm gold particles, as shown in Figure 6. Trimers were prepared using 5-nm Au−**B′H** and 10-nm Au−**HA′** conjugates and an $\mathbf{AB_2}$ scaffold. Tetramers were prepared using scaffolds $\mathbf{A'B_2}$ and $\mathbf{AC_2}$, along with 10-nm Au−**B′H** and 5-nm Au−**C′N**. The electrophoretic behavior of asymmetric assemblies has not yet been investigated in detail but is expected to be more complex, since more types of partial assemblies are possible and 5- and 10-nm conjugates impact structure migration differently. Further, since 5- and 10-nm Au particles have different extinction coefficients, band optical density is more difficult to correlate with the number of structures present in the band. In each asymmetric structure sample, the highest band was extracted from the agarose gel and analyzed by TEM (Figure 6 and Supporting Information). The target assemblies were present in micrographs for both the trimer and tetramer structures, in addition to lower-order structures and aggregates. Future experiments will utilize asymmetric assemblies to further probe the conformations adopted at flexible points in the structure.

Conclusion

Branched DNA scaffolds and gold nanoparticles conjugated to single strands of thiolated linear DNA have been hybridized to give discrete nanoparticle trimers and tetramers of controlled composition, as evidenced by gel electrophoresis and TEM. Three tetramer architectures were investigated, and though the extended architecture resulted in the highest degree of conjugate hybridization, both external-hairpin and extended conformations produced tetramer assemblies in similar yields as measured by gel band intensities. Micrographs from extracted gel bands show that a large majority of particles from each band participate in a single type of grouping (tetramers, trimers, dimers, etc.), suggesting that each discrete band in the gel corresponds to a specific structure type and indicating that development of an optimized band extraction procedure will make gel electrophoresis purification appropriate for isolation of a variety of nanoparticle assemblies.

Ongoing experiments focus on increasing tetramer yield and forming a bistable DNA−Au structure through covalent cross-linking of scaffolds and conjugates. Cross-linking of exterior hairpins may also provide a means to achieve accurate close placement of even larger nanoparticles, which currently require long conjugate sequences (>100 bases) for monoconjugate purification. Additionally, use of a more rigid branching moiety in the scaffold will reduce conformational flexibility, resulting in more predictable structure geometry. Optical experiments will be performed on assemblies in solution, using dark-field microscopy to probe the plasmon coupling behavior of trimer and tetramer structures.

Acknowledgment. The Center for New Directions is supported by Bristol-Myers Squibb as a Sponsoring Member and Novartis as a Supporting Member. Financial support of this work by the Biomolecular Program of LBNL, U.S. Department of Energy under Contract No. DE-AC03-76SF00098 is gratefully acknowledged. This material is based in part upon work supported by the National Science Foundation under Grant No. EIA-0121368. S.A.C. and C.M.M. gratefully acknowledge an NSF-IGERT Predoctoral Fellowhsip and a Howard Hughes Medical Institute Predoctoral Fellowship, respectively.

Supporting Information Available: Tetramer band identification experiment, TEM statistics from extracted tetramer hybridization bands, additional TEM images, and tetramer diameter data for external-hairpin and extended structures. This material is available free of charge via the Internet at http://pubs.acs.org.

CM0484089